

Article

# An Assessment of Two Models of Wave Propagation in an Estuary Protected by Breakwaters

Amin Ilia <sup>1,\*</sup> and James O'Donnell <sup>2</sup>

<sup>1</sup> Department of Marine Sciences, University of Connecticut, Groton, CT 06340, USA; [amin.ilia@uconn.edu](mailto:amin.ilia@uconn.edu)

<sup>2</sup> Department of Marine Sciences, University of Connecticut, Groton, CT 06340, USA;

[james.odonnell@uconn.edu](mailto:james.odonnell@uconn.edu)

\* Correspondence: [amin.ilia@uconn.edu](mailto:amin.ilia@uconn.edu); Tel.: +1-631-933-5683

**Abstract:** Breakwaters influence coastal wave climate and circulation by blocking and dissipating wave energy. Accurate representation of these effects is essential to the determination of coastal circulation and wave processes. MIKE21SW and SWAN are two third-generation spectral wave models which are used widely in coastal research and engineering applications. Recent improved versions of the models are able to consider the influence of breakwater structures. In this study, we used available observations to evaluate the accuracy of model simulations of waves in New Haven Harbor, Connecticut, USA, an estuary with three detached breakwaters near the mouth. We then compare the accuracy and computational efficiency of MIKE21SW and SWAN. Both models were executed on the same unstructured triangular grid. The boundary conditions were derived from a bottom mounted ADCP on the offshore side of the breakwaters. Wind forcing was applied using data from the Central Long Island Sound buoy. We find that both models are largely consistent with observations during storms. The MIKE21SW significant wave height and wave direction simulations were slightly superior; however, SWAN is more efficient and faster due to its implementation of a fully implicit technique for time integration.

**Keywords:** Wave hindcast; Breakwater; Harbor; Estuary; SWAN; MIKE21SW; Assessment

## 1. Introduction

Breakwaters are used to protect harbors and shorelines from waves and to limit coastal erosion. In harbors, coastal breakwaters provide tranquility to ease both navigation and berthing for vessels. Breakwaters influence coastal wave climate by breaking, reflecting, and diffracting wave energy. Studying these influences in situ poses a challenge. In recent years, spectral wave models have become more widely used and important tools to understand coastal wave behavior. However, the performance and precision of the spectral models in the presence of the breakwaters are not well examined.

SWAN, MIKE21SW, and Wavewatch III are three commonly used spectral wave models in coastal and ocean communities. Wavewatch III is mostly used for deep ocean and open sea applications and is not able to include breakwater structures. On the other hand, the recent versions of SWAN and MIKE21SW are equipped to handle breakwaters. In this study, we employed SWAN (v41.20) and MIKE21SW (v2017) to simulate the effects of three coastal breakwaters on the wave field in New Haven Harbor, Connecticut, and then assessed their accuracy and efficiency.

Previously, Strauss et al. [1] compared simulations of waves on a narrow continental shelf in Gold Coast, Australia in SWAN and MIKE21SW. SWAN was executed in the fully spectral mode with a structured grid, while MIKE21SW was executed on directional decoupled parametric mode with an unstructured grid. The results indicated that both models overestimated significant wave

height in enabled wind forcing. Moeini and Etemad-Shahidi [2] applied SWAN and MIKE21SW for hindcasting waves in Lake Erie. The study suggested SWAN simulates significant wave height better, while MIKE21SW simulates wave period and direction better. Conversely, Fonseca et al. [3] suggested that MIKE21SW, SWAN, and STWAVE models have similar behavior and precision when examining performance on the Portuguese coast. Hoque et al. [4] evaluated SWAN and MIKE21SW in the Mackenzie Delta in Beaufort Sea, Canada. They concluded that the results of the models are almost identical in shallow water, but in water shallower than 7m, SWAN simulated the significant wave height better, though the peak period from MIKE21SW was superior.

In all previous studies, SWAN was executed on a structured grid and MIKE21SW on an unstructured grid. In this study, for the first time, both SWAN and MIKE21SW were run on the same unstructured grid and evaluated inside a harbor in the presence of breakwaters. The models were used to simulate waves in New Haven Harbor, which is partially sheltered by three detached breakwaters at the connection to Long Island Sound (Figure 1). The model results were compared to data from a bottom mounted Acoustic Doppler Current Profiler (ADCP) in the harbor. The results and the efficiency of the models were analyzed to determine their strengths and weaknesses. In addition, possible explanations for their differences were discussed.

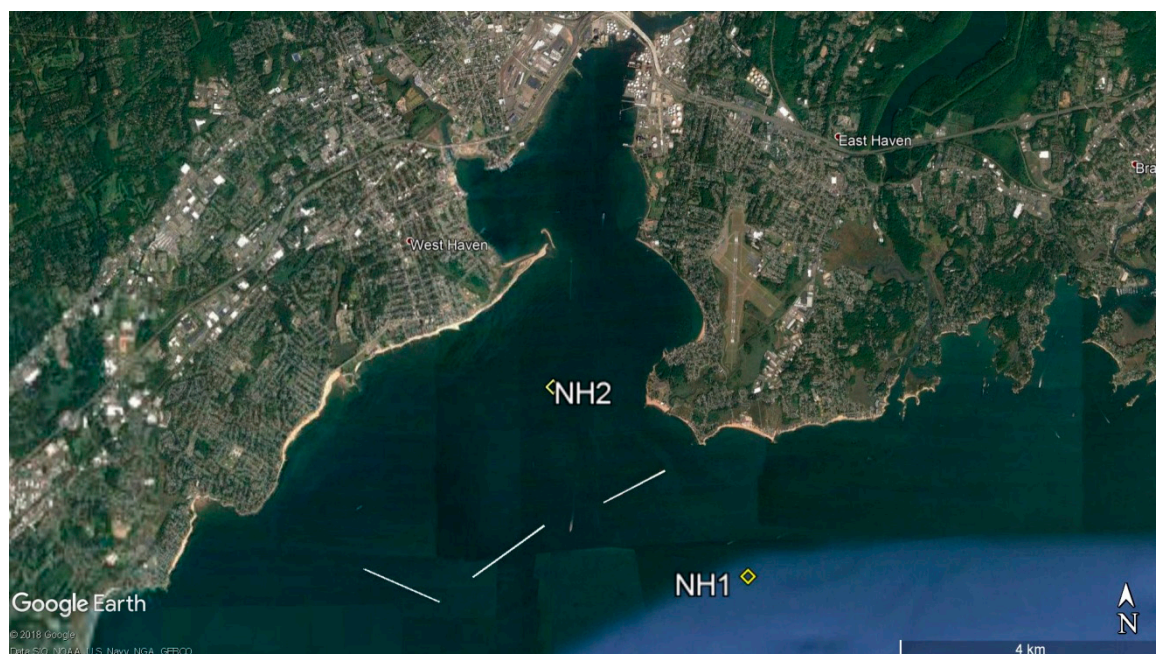


**Figure 1.** Locations of breakwater structures in front of New Haven Harbor are highlighted by white lines and ADCP locations inside and outside the harbor highlighted by yellow boxes and labels. (Image Source: "New Haven Harbor". 41° 15'03.79" N and 72° 55'20.36" W . Google Earth. September 23, 2017. June 18, 2018)

## 2. Model Descriptions

MIKE21SW is a proprietary model developed by DHI Company. It is one of the most widely used wave models in coastal and marine engineering projects around the world. It has a Graphical User Interface (GUI) that makes it simple to set up the model and visualize the results. SWAN is an open source model developed by the Delft University of Technology. It is often used in academic coastal research and has been integrated to community circulation models. For simplification and clarification, we introduce the models by summarizing their similarities and differences.

SWAN [5], and MIKE21SW [6] are both 3rd generation fully spectral wave models. The models solve the wave action balance equation, described by Mei [7], Komen et al [8], and Young [9]. In Cartesian coordinates without ambient current, the wave action balance equation can be written as:

$$\frac{\partial N}{\partial t} + \nabla \cdot (\vec{c}_g N) = \frac{S}{\sigma} \quad (1)$$

Where  $N(x, \sigma, \theta, t)$  is the wave action density,  $\vec{c}_g = (c_x, c_y, c_\sigma, c_\theta)$  is the wave group velocity,  $\sigma$  is relative frequency,  $\theta$  is wave direction,  $t$  is time, and  $S$  is the total source and sink terms which represent generation, dissipation and redistribution of wave energy.  $\nabla$  is the four dimensional differential operator with respect to  $x, y, \sigma$ , and  $\theta$ .

The source terms in both models are almost the same. Wave dissipation terms such as bed friction, wave breaking, whitecapping, nonlinear quadruplet interactions, nonlinear triad wave interactions, and diffraction are the same or very similar. However, in some cases such as wind input, whitecapping and quadruplet wave interaction, SWAN is able to support more methods and coefficients.

SWAN can be run on both structured and unstructured grids, while MIKE21SW only uses unstructured grids. The spatial discretization method differs between the models. SWAN's spatial discretization is based on a vertex-centered method while MIKE21SW uses a cell-centered method. This implies that wave action  $N$  is stored at the grid cell vertices in SWAN and at the cell center in MIKE21SW. Thus, the control volume in SWAN is a polygon, while in MIKE21SW it is triangular.

The methods for time integration drastically differ between the models. MIKE21SW uses Euler explicit scheme in the propagation term, while SWAN uses Euler fully implicit method. Because the computational scheme of MIKE21SW is explicit, it avoids solving a large system of equations; however, the downside is that the temporal step is limited by the Courant number. On the other hand, in SWAN's fully implicit scheme, the temporal step is not limited and the computation is stable for any time step, but in this case a large system of equations must be solved to achieve a solution. These differences in the time integration method can impact the model efficiency, as well as the computational accuracy.

### 3. Methods

In this study, the model domain is New Haven Harbor, Connecticut, USA. New Haven Harbor is located in Long Island Sound, a large estuary on the northeast coast of the United States. There are three detached breakwaters in front of the harbor to protect it from excessive waves during extreme storms. The area is frequently affected by strong winds during winter, from January to March, and occasionally by hurricanes in the summer and early fall. The significant wave height in central Long Island Sound, where New Haven Harbor is located can exceed two meters. To observe the effect of breakwaters on waves in extreme storms, we deployed two ADCPs in New Haven Harbor, one outside the harbor (NH1) and one inside (NH2), during the winter of 2015 from January 21st to April 5th. The wind data were gathered during the same period by the Central Long Island Sound Buoy (CLIS) which is located 25 km from New Haven. Depths and locations of the observations can be found in Table 1, and Figure 1 illustrates the field site.

**Table 1.** Location and depth information for the observations used for modeling

| Station ID | Latitude (N) | Longitude (W) | Depth (m) | Location       |
|------------|--------------|---------------|-----------|----------------|
| NH1        | 41° 13.44'   | 72° 53.15'    | 10.4      | Outside Harbor |
| NH2        | 41° 14.64'   | 72° 56.96'    | 5.2       | Inside Harbor  |
| CLIS       | 41° 8.28'    | 72° 39.30'    | 27        | Outside Harbor |

Instead of applying a nesting approach, which uses results from a large-scale model to force the boundaries of the local wave model, we used observed wave data at NH1 to force the open boundary of the models. In this way, we can eliminate the possible uncertainty from the large-scale model adding to the local model. The models were also forced by a uniform wind stress over the domain at half hour intervals using observation from the CLIS buoy.



For the results from the models to be comparable, both models were set up with the same configurations and forcing condition as much as possible. Using a grid converter, available in the MIKE21 package, we were able to run both models with the same unstructured triangulate grid which was generated by Surface-water Modeling System package (SMS v12), as shown in Figure 2. The grid was smoothly refined around the breakwaters and inside the harbor. Some minor differences in the configuration could not be eliminated. For each model, we tested settings and coefficients, and applied the set that achieved the best agreement with the observations.

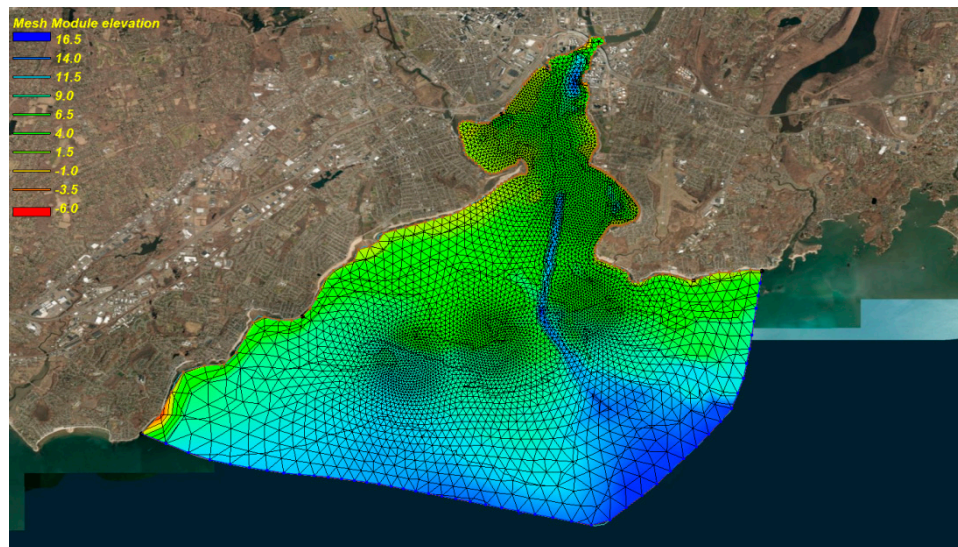


**Figure 2.** Unstructured triangulate grid used for both SWAN and MIKE21SW; the grid was smoothly refined around the breakwaters and inside the harbor

Both models were executed in 3rd generation fully spectral and non-stationary mode. The same spectral discretization (25 frequencies and 16 directional discretizations) were applied to SWAN and MIKE21SW with a minimum frequency of 0.06 Hz and a maximum of 0.59 Hz.

Wind input source and whitecapping dissipation functions are different in the models. SWAN is configured to use the wind input source function of Janssen [10, 11], as implemented in WAM cycle 4 [12]; the method of Komen [13], as implemented in WAM cycle 3 [14]; and method of Yan [15]. MIKE21SW only supports Janssen's method. Dissipation through whitecapping is based on the development of Hasselmann [16] in both Janssen's and Komen's methods, however, the coefficients are different (see Komen [8, 13]). Yan's wind input method is combined with saturation-based whitecapping as described in Van der Westhuysen [17, 18]. Moeini and Etemad-Shahidi [2] suggested that Komen's method led to more accurate significant wave height than Janssen's method for Lake Erie. Hoque [4] indicated Westhuysen's formulation tends to have better significant wave height in the Mackenzie Delta. We tested all three methods with SWAN. We found that Janssen's method provides the best wave height simulations in the harbor. Therefore, Janssen's wind input method was used for both models with the tunable coefficients set as  $C_{ds}^* = 4.5$  and  $\delta = 0.5$ .

Wave dissipation due to bottom friction was represented in both models by the empirical JONSWAP [19] approach. The friction coefficients introduced by Zijlema et al. [20] were used:  $C_b = 0.038 \text{ m}^2 \text{ s}^{-3}$  and  $c_{fw} = 0.0077 \text{ ms}^{-1}$ .

Waves breaking in shallow water was taken into account in the models using the Battjes and Janssen [21] formulation with  $\alpha = 1$  and  $\gamma = 0.8$ . Also, triad wave-wave interactions were enabled in both models. Triad interactions in MIKE21SW are calculated based on Eldeberky and Battjes [22] and in SWAN based on Eldeberky [23], a slightly modified version of the former. Quadruplet wave-wave interactions were also enabled in the models. In both models, the quadruplet wave-wave interactions are computed with the Discrete Interaction Approximation (DIA) as proposed by Hasselmann et al [24].

In the case of breakwater structures present, diffraction computations become important. Diffraction is taken into account in the models using a phase-decoupled refraction-diffraction approximation proposed by Holthuijsen et al. [25]. Diffraction computation in the models is almost the same, but a wave field smoothing technique for the computation of the diffraction parameter that is not available in SWAN with an unstructured grid.

4. Results

The results of SWAN and MIKE21SW models were compared and assessed inside the harbor at NH2 during storms when the wave heights were large. We divided the observations into five storm periods, detailed in Table 2. Each of these periods is discussed separately, and then the results are summarized. The statistical parameters used for data validation are:

$$\text{Bias}(\text{error}) = \frac{\sum_{i=1}^n (Y_i - X_i)}{n}, \tag{2}$$

$$\text{RMS} = \sqrt{\frac{\sum_{i=1}^n (Y_i - X_i)^2}{n}}, \tag{3}$$

$$m = \text{slope of the best fitted line}, \tag{4}$$

$$R^2 = 1 - \frac{\sum_{i=1}^n (Y_i - Y'_i)^2}{\sum_{i=1}^n (Y_i - \bar{Y})^2}, \tag{5}$$

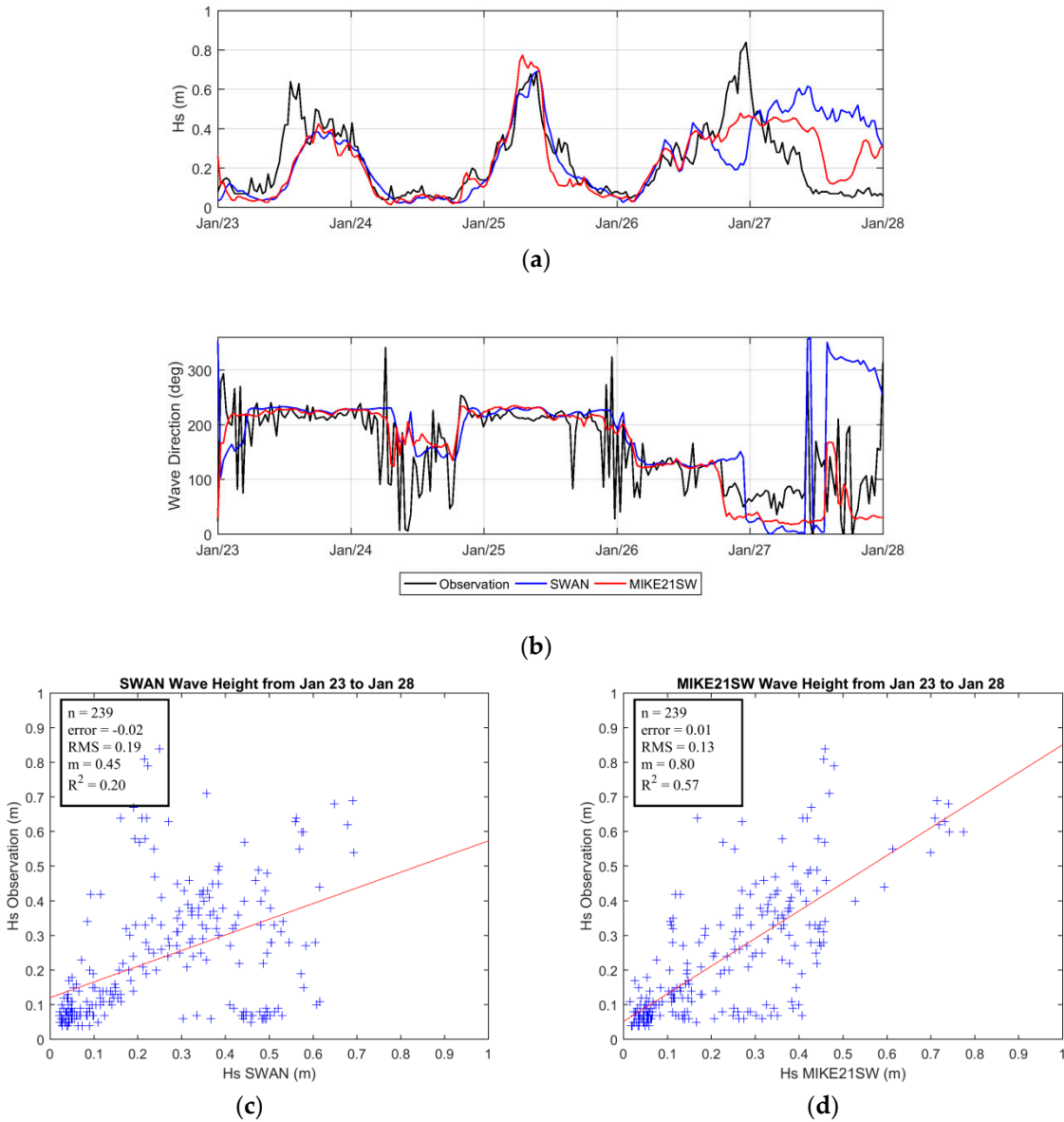
where  $Y_i$ , with mean  $\bar{Y}$ , are the observed values,  $X_i$  are the simulated values, and  $n$  is the number of data points.  $RMS$  is the root mean square error,  $R^2$  is the fraction of the variance in the data explained by the model,  $Y'_i$  is the estimated value by regression, and  $\bar{Y}$  is the mean of the observed values.

Table 2. Storm periods used for analyzing and assessing the models

| No. | Storm Period      |
|-----|-------------------|
| 1   | January 23 to 28  |
| 2   | February 01 to 10 |
| 3   | February 14 to 21 |
| 4   | March 06 to 08    |
| 5   | April 01 to 05    |

Three consecutive high wind intervals occurred during the first storm period, Jan. 23 to 28. Comparison between observations and the models of significant wave height and wave direction, as well as scatter plots and statistical analysis for Storm Period 1 are presented in Figure 3. For the first storm, the models' significant wave height ( $H_s$ ) results are very similar to each other and both miss the first part of the storm peak (Figure 3a). Also, both models are able to simulate wave direction correctly (Figure 3b). For the second storm, both models reproduce the storm's entire wave height peak, but MIKE21SW overestimates the peak storm wave height a little. Simulated wave direction for the second storm also agrees well with the observations. For the third storm, the fidelity of the models is poor. The SWAN results are worse than MIKE21SW and the correlation between SWAN significant wave heights and the observed series is negative. Further, neither model reproduces the decrease in significant wave height at the end of the storm. The wave direction results from the models explain the model's failure. In the presence of breakwaters, waves enter the harbor from particular directions defined by breakwater orientation. Therefore, an error in simulating wave direction can drastically change the wave field in the harbor. In our case, after Jan 26, 6:00pm, both models have erroneous wave directions, and since the interior is sensitive to this direction, the error

in direction leads to a large error in the wave field in the harbor. The statistical parameters show that MIKE21SW results are better than SWAN for this period. *Bias* and *RMS* errors in significant wave heights obtained from MIKE21SW (Figure 3c) are less than those in SWAN (Figure 3d).  $R^2$  for SWAN is very low due to negative correlation between modeled and observed wave height for the third storm.



**Figure 3.** Comparison of SWAN (blue), MIKE21SW (red), and observation (black) inside the harbor for the time interval of Jan 23 to 28. (a): Significant wave height comparisons. (b): Wave direction comparison. (c): Scatter plot and statistical parameters for SWAN. (d): Scatter plot and statistical parameters for SWAN. Both visually and statistically MIKE21SW results are better than SWAN for the time interval of Jan 23 to 28.

Comparison of the results of the models and observations from Storm Period 2, February 1 to 10, are shown in Figure 4. Both models overestimated the strongest storm significant wave height on February 2, however, SWAN overestimated it more than MIKE21SW (Figure 4a). There is some error in simulated wave direction and wave height on February 5 and 6 (Figure 4b). Again, an error in simulation of wave direction changes the wave field in the harbor and causes error in significant wave height. In this case, SWAN error is larger than that in MIKE21SW. Otherwise, the models' performance are the same in the other storms. Both missed some small oscillations and

overestimated others. MIKE21SW performs statistically better than SWAN once again (Figure 4c and 4d).

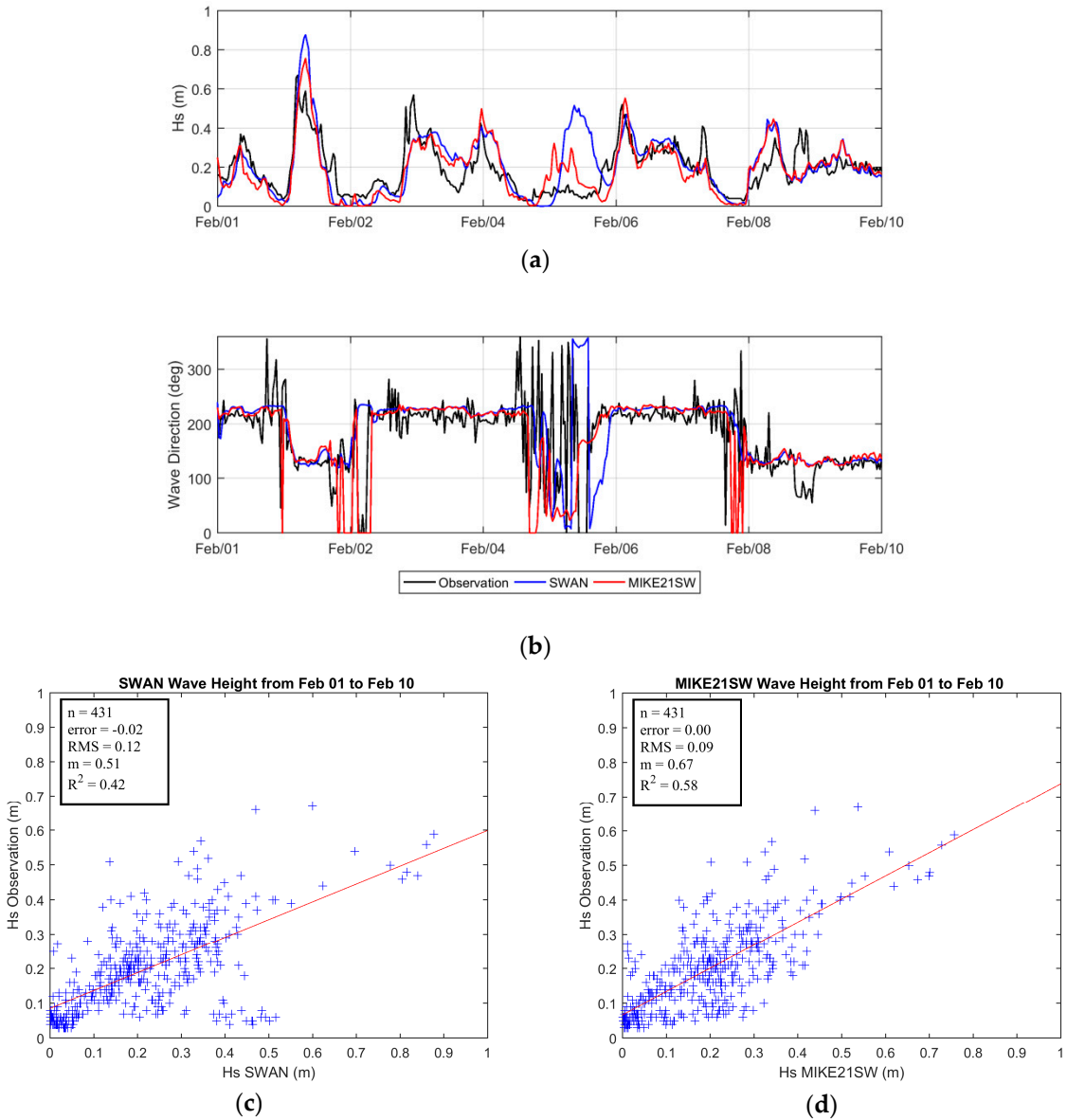


**Figure 4.** Comparison of SWAN (blue), MIKE21SW (red), and observation (black) inside the harbor for the time interval of Feb.1 to 10. (a): Significant wave height comparisons. (b): Wave direction comparison. (c): Scatter plot and statistical parameters for SWAN. (d): Scatter plot and statistical parameters for MIKE21SW. Both visually and statistically MIKE21SW results are better than SWAN for the time interval of Feb. 1 to 10.

Three storms occurred in the third period, from Feb. 14 to 21. As shown in Figure 5, the models accurately simulate the first storm. During the second storm, MIKE21SW accurately simulates significant wave height in the first part of the storm but later produces overestimates. In contrast, SWAN overestimates significant wave height over the whole storm duration. For the third storm, both models successfully simulate the wave height and direction. Overall, *bias* and *RMS* errors are lower and the slope of the best-fitted line and *R*<sup>2</sup> are higher for MIKE21SW, (Figure 5c and 5d). Therefore, MIKE21SW results are more accurate than SWAN for this time period. Error in the simulated wave direction is apparent, particularly in SWAN results.

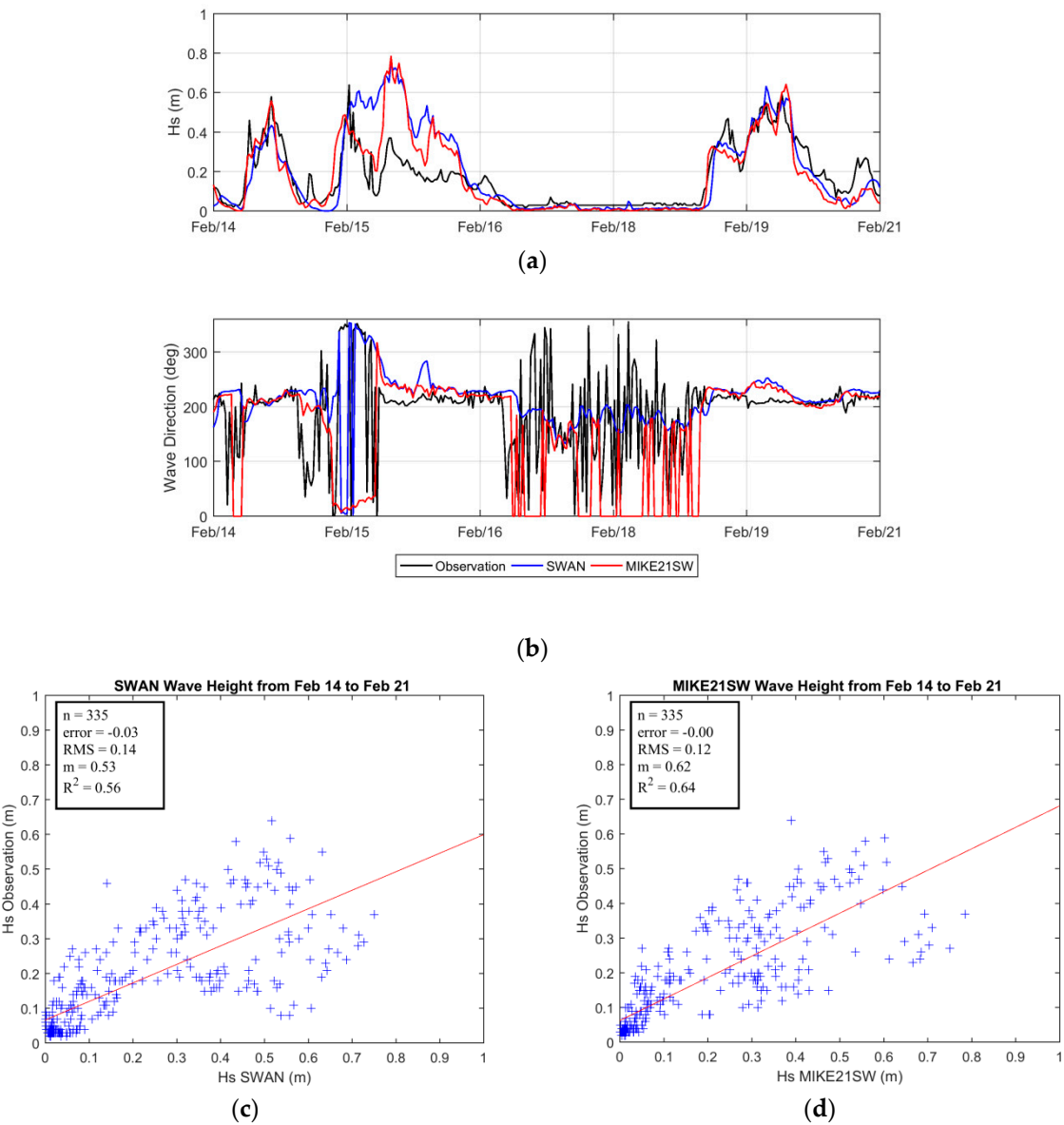


**Figure 5.** Comparison of SWAN (blue), MIKE21SW (red), and observation (black) inside the harbor for the stormy period of Feb 14 to 21. (a): Significant wave height comparisons. (b): Wave direction comparison. (c): Scatter plot and statistical parameters for SWAN. (d): Scatter plot and statistical parameters for MIKE21SW. Both visually and statistically MIKE21SW results are better than SWAN for the time interval of Feb 14 to 21.

In the fourth storm period, both models fail to correctly simulate significant wave height variations between March 6 and 8, as shown in Figure 6. The storm includes two peaks in significant wave height, but the models underestimated both (Figure 6a). However, they correctly estimate wave directions (Figure 6b) and the statistical parameters show similar model performance. Some statistical parameters are better for MIKE21SW and others for SWAN (Figure 6c and 6d). Generally, the results of both models were poor for this storm.



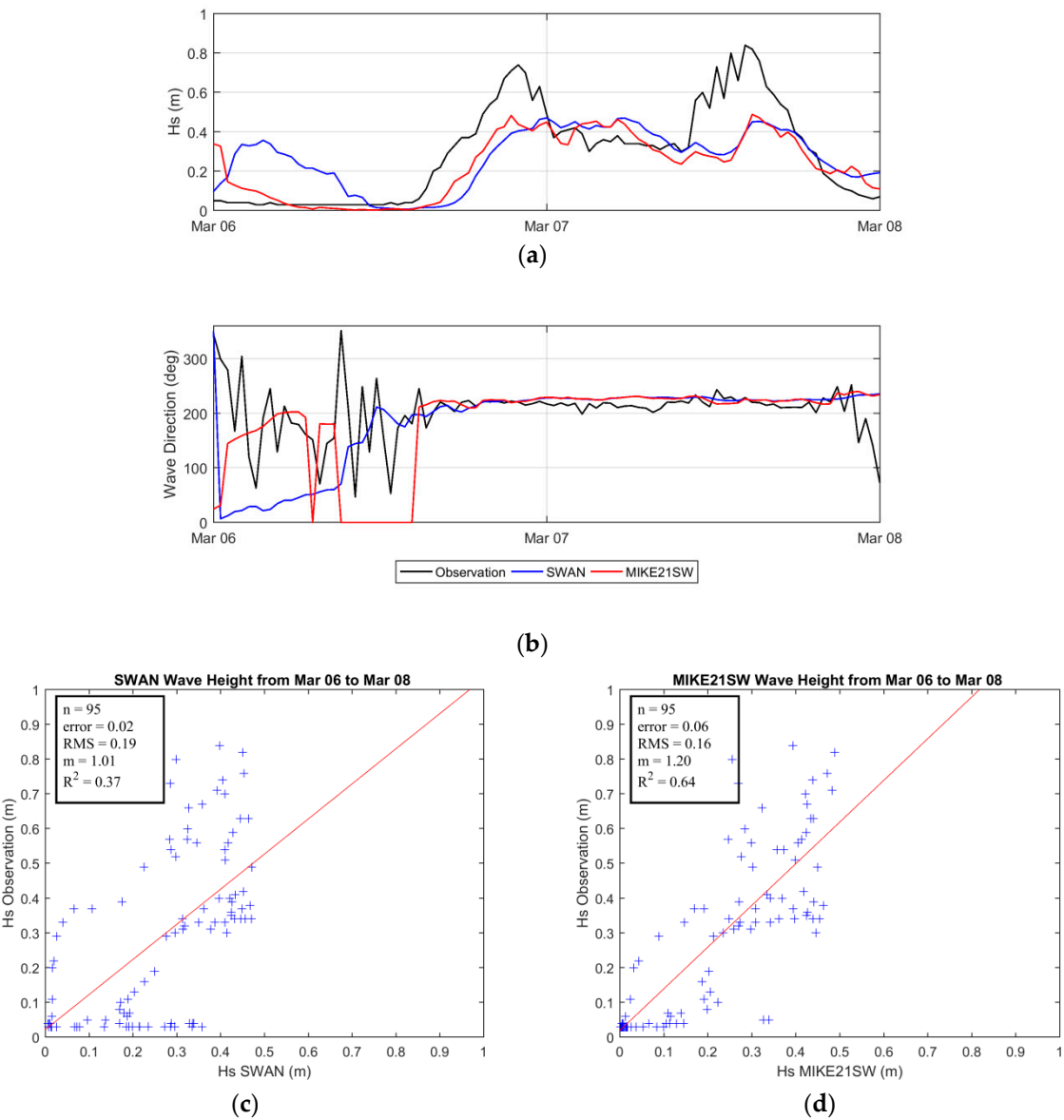


**Figure 6.** Comparison of SWAN (blue), MIKE21SW (red), and observation (black) inside the harbor for the stormy period of March 06 to 08. (a): Significant wave height comparisons. (b): Wave direction comparison. (c): Scatter plot and statistical parameters for SWAN. (d): Scatter plot and statistical parameters for SWAN. Both models didn't do well during this time interval.

Results from Storm Period five are illustrated in Figure 7, showing the assessment of the models results during the storm took place on April 2 and 3. MIKE21SW is able to catch the storms highest wave height and correctly compute wave direction during the storm. SWAN results are also suitable, but it underestimates the storm peak and there is a delay in storm growth (Fig 7a and 7b). Except for the slope of the best-fitted line, statistical parameters are better for MIKE21SW results (Figure 7c and 7d).

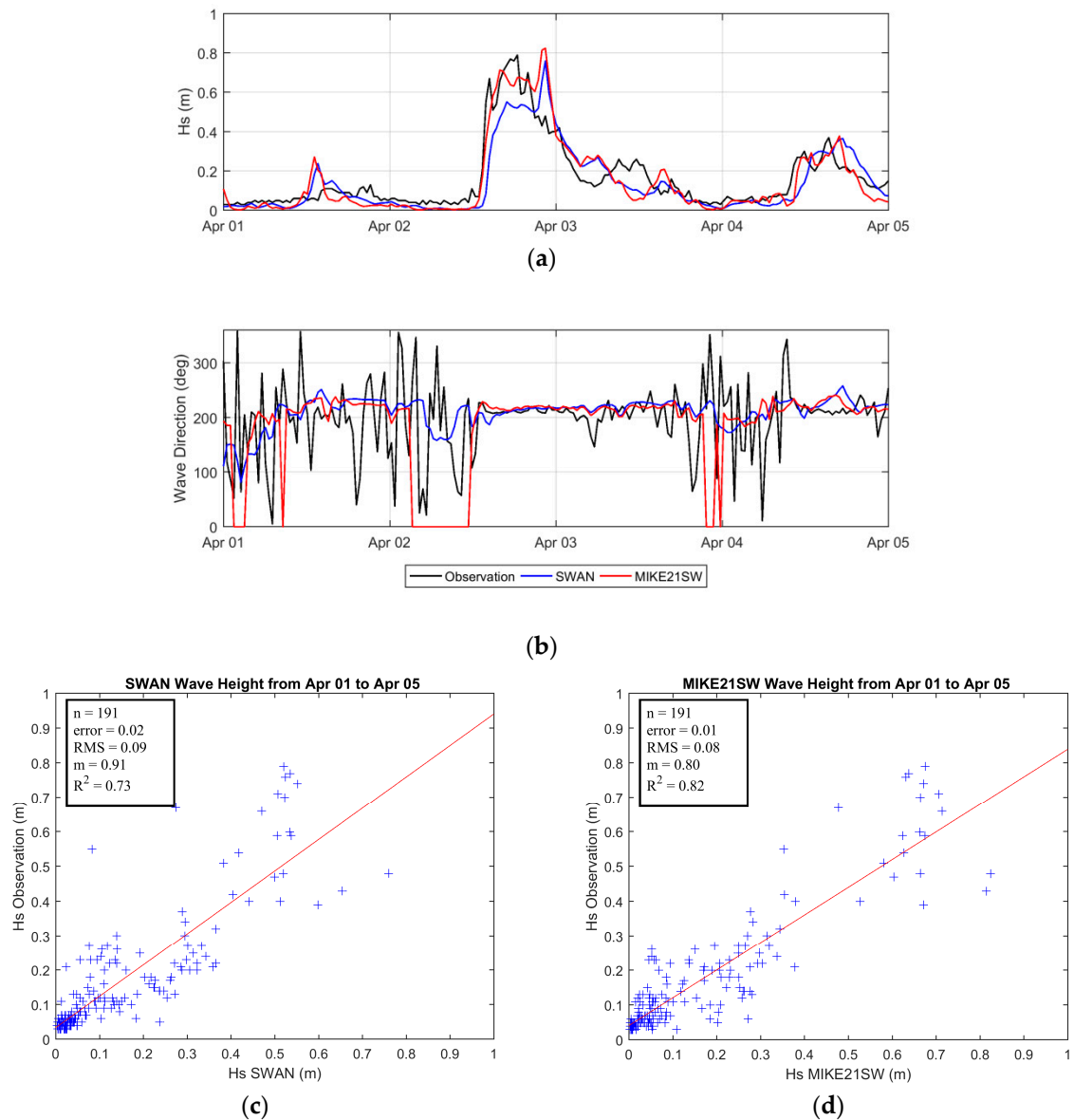


**Figure 7.** Comparison of SWAN (blue), MIKE21SW (red), and observation (black) inside the harbor for stormy period of April 01 to 05. (a): Significant wave height comparisons. (b): Wave direction comparison. (c): Scatter plot and statistical parameters for SWAN. (d): Scatter plot and statistical parameters for MIKE21SW. Both models did not do well during this time interval.

Finally, we analyzed all storms together as presented in Figure 8. *Bias* for both models is 0.01 with opposite signs. *RMS* of MIKE21SW is 0.04 (27%) lower than *RMS* obtained from SWAN results. The slope of best-fitted line for MIKE21SW is closer to one. *R<sup>2</sup>* of MIKE21SW results is 0.20 higher than the results of SWAN. Therefore, the results suggest MIKE21SW more precisely simulates wave height and wave directions in the harbor during storms, although the models results have a lot of similarity.

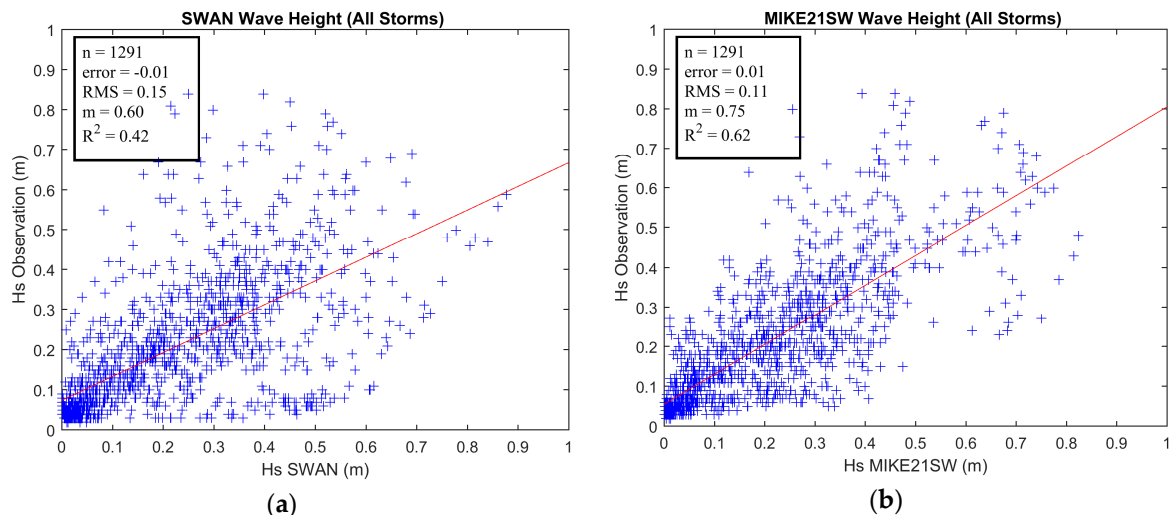


**Figure 8.** Comparison of scatter plot and statically parameter between SWAN (a) and MIKE21SW (b) for all storms. The statistical parameters suggest that MIKE21SW model is more precise than SWAN model.

## 5. Discussion

Although the models have similar predictions, in some cases MIKE21SW more accurately simulates wave height and direction north of the breakwaters in New Haven Harbor. The MIKE21SW model provides superior simulations of wave direction, growth and decay of the significant wave height during storms, and the peak wave heights. The differences in model performance are not associated with the open boundary conditions or wind forcing, since the same values are used in the two models, and must be attributed to the model formulation.

Besides the accuracy of the model, the efficiency and simplicity of the models are important in assessment of the model utility. Because MIKE21SW has a GUI, setting up, executing, extracting, and visualizing the results is easier than SWAN. SWAN, on the other hand, is much more efficient computationally than MIKE21SW. SWAN executes the same model grid and configuration using the same computational engine about nine times faster than MIKE21SW. The high computational efficiency of SWAN accelerates the calibration and validation of the model and would allow additional grid refinement to improve its accuracy. To assess this, we doubled the grid resolution in SWAN and reran it from Feb. 1 to 10. The SWAN results improved with respect to error in wave direction and wave height, but did not change in the case of overestimating and underestimating the storm wave height peaks. Even with a higher grid resolution, the MIKE21SW results appear to be slightly better than SWAN.

We believe that the time integration method employed in SWAN and MIKE21SW play the main role in determining the differences in the results and efficiency. MIKE21SW uses an explicit Euler scheme when computing wave propagation while SWAN uses a fully implicit method. This study suggests that the implicit method, used in SWAN, is computationally much more efficient than explicit method, used in MIKE21SW, because of the restriction imposed by the Courant number on the temporal step in the explicit method. In addition, SWAN uses a point-by-point multi-directional Gauss-Seidel iteration technique that circumvents the need to construct and solve a large system of equations as is typical in implicit methods [26]. This technique highly improves the computational efficiency of SWAN model.

## 6. Conclusions

SWAN and MIKE21SW are two spectral wave models that solve the wave action balance equations. Although there are lots of similarities in both the main equations and wave source terms, they have some minor differences in the algorithms used to obtain solutions that impact both the results and efficiency of the models. For the first time, SWAN and MIKE21SW were assessed on the

same unstructured grid and inside a harbor in the presence of three detached breakwaters. This study suggests the results of the models are consistent with observations during the majority of storms. The models behave similarly in most events, but in some circumstances, when waves arrive from particular directions defined by the orientation of the breakwaters, MIKE21SW more accurately simulates significant wave height and wave direction than SWAN. The errors in SWAN lead to both overestimates and underestimates in wave height, incorrect wave direction, and delays in wave high trends. SWAN is, however, computationally more efficient than MIKE21SW, because it uses a fully implicit method and Gauss-Seidel iteration technique for solving the wave action balance equations. Refining the grid size in SWAN improved its results, but are still slightly less accurate than MIKE21SW with a larger grid size.

**Author Contributions:** Conceptualization, A.I. and J.O'D.; Methodology, A.I.; Software, A.I.; Validation, A.I. and J.O'D.; Formal Analysis, A.I.; Investigation, A.I. and J.O'D.; Resources, A.I.; Writing-Original Draft Preparation, A.I.; Writing-Review & Editing, A.I. and J.O'D.; Visualization, A.I.; Supervision, J.O'D.; Project Administration, J.O'D.; Funding Acquisition, J.O'D.

**Funding:** The observations in this research were funded by NOAA and the Connecticut Department of Energy and Environmental Protection.

**Acknowledgments:** We are grateful to DHI for providing us with the MIKE21 package. Connecticut Institute for Resilience and Climate Adaptation (CIRCA) supported the observations with funding from NOAA and the Connecticut Department of Energy and Environmental Protection. We are also grateful to Kay Howard-Strobel, Ale Cifuentes and Molly James for valuable technical assistance.

**Conflicts of Interest:** The authors declare no conflict of interest.



## References

1. Strauss, D.; Mirferendesk, H.; Tomlinson, R. Comparison of two wave models for Gold Coast, Australia. In: Lemckert, C. (ed.), Proceedings of the 9th International Coastal Symposium. *Journal of Coastal Research*, **2007**, Special Issue No. 50, pp. 312–316.
2. Moeini, M. H.; Etemad-Shahidi, A. Application of two numerical models for wave hindcasting in Lake Erie. *Applied Ocean Research* **2007**, *29*, 137–145.
3. Fonseca, R. B.; Gonçalves, M.; Guedes Soares, C. Comparing the Performance of Spectral Wave Models for Coastal Areas. *J. Coast. Res.* **2017**, 331–346, DOI: 10.2112/JCOASTRES-D-15-00200.1.
4. Hoque, M. A.; Perrie, W.; Solomon, S. M. Evaluation of two spectral wave models for wave hindcasting in the Mackenzie Delta. *Applied Ocean Research*, **2017**, *62*, 169–180.
5. Booij, N.; Ris, R. C.; Holthuijsen, L. H. A third-generation wave model for coastal regions: 1. model description and validation. *Journal of Geophysical Research: Oceans*, **1999**, *104*, 7649–7666, doi:10.1029/98JC02622
6. DHI group. MIKE 21 Spectral Wave Module. Scientific Documentation. Danish Hydraulic Institute (DHI), 2017, 56p.
7. Mei, C. C. The applied dynamics of ocean surface waves. Volume 1 of Advanced series on ocean engineering, World Scientific, 1989, ISBN 9971507897
8. Komen, G. J.; Cavaleri, L.; Donelan, M.; Hasselmann, K.; Hasselmann, S.; Janssen, P. A. E. M. *Dynamics and Modelling of Ocean Waves*; Cambridge University Press: Cambridge, 1994; .
9. Young, I.R. Wind Generated Ocean Waves, Elsevier Ocean Engineering Series, Volume 2, 1st Edition, Eds. R. Bhattacharyya and M.E. McCormick, Elsevier, 1999, ISBN: 9780080433172
10. Janssen, P. A. E. M. Wave-Induced Stress and the Drag of Air Flow over Sea Waves. *J. Phys. Oceanogr.* **1989**, *19*, 745–754, DOI: 10.1175/1520-0485(1989)019<0745:WISATD>2.0.CO;2.
11. Janssen, P. A. E. M. Quasi-linear Theory of Wind-Wave Generation Applied to Wave Forecasting. *J. Phys. Oceanogr.* **1991**, *21*, 1631–1642, DOI: 10.1175/1520-0485(1991)021<1631:QLTOWW>2.0.CO;2.
12. Gunther, H.; Hasselmann, S.; Janssen, P.A.E.M. The WAM model Cycle 4 (revised version), Deutsch. Klim. Rechenzentrum, Techn. Rep. No. 4, Hamburg, Germany, 1992.
13. Komen, G. J.; Hasselmann, K.; Hasselmann, K. On the Existence of a Fully Developed Wind-Sea Spectrum. *J. Phys. Oceanogr.* **1984**, *14*, 1271–1285, DOI: 10.1175/1520-0485(1984)014<1271:OTEOAF>2.0.CO;2.
14. WAMDI Group. The WAM Model—A Third Generation Ocean Wave Prediction Model. *Journal of Physical Oceanography*, **1988**, *18*, 1775–1810
15. Yan, L. An Improved Wind Input Source Term for Third Generation Ocean Wave Modelling. Scientific report WR-No 87-8, De Bilt, The Netherlands. **1984**.
16. Hasselmann, K. On the spectral dissipation of ocean waves due to white capping. *Bound. -Layer Meteorol.* **1974**, *6*, 107–127, DOI: 10.1007/BF00232479.
17. Van der Westhuysen, A.J. Advances in the spectral modelling of wind waves in the nearshore, Ph.D. thesis, Delft University of Technology, Department of Civil Engineering, The Netherlands, 2007.
18. Van der Westhuysen, A. J.; Zijlema, M.; Battjes, J. A. Nonlinear saturation-based whitecapping dissipation in SWAN for deep and shallow water. *Coastal Engineering* **2007**, *54*, 151–170.
19. Hasselmann, K.; Barnett, T.P.; Bouws, E.; Carlson, H.; Cartwright, D.E.; Enke, K.; Ewing, J.A.; Gienapp, H.; Hasselmann, D.E.; Kruseman, P.; Meerburg, A.; Müller, P.; Olbers, D.J.; Richter, K.; Sell W.; Walden, H. Measurements of wind-wave growth and swell decay during the Joint North Sea Wave Project (JONSWAP), Deutsches Hydrographisches Institut, Ergänzungsheft 8-12, 1973.
20. Zijlema, M.; van Vledder, G. P.; Holthuijsen, L. H. Bottom friction and wind drag for wave models. *Coastal Engineering* **2012**, *65*, 19–26.
21. Battjes, J.A.; Janssen, J.P.F.M. Energy loss and set-up due to breaking of random waves, Proc. 16th Int. Conf. Coastal Engineering, Hamburg, Germany, August 27–September 3, 1978, ASCE, p569–587, doi:doi:10.1061/9780872621909.034
22. Eldeberky, Y.; Battjes, J.A. Parameterization of triad interactions in wave energy models, Proc. Coastal Dynamics Conf. '95, Gdansk, Poland, 1995, 140–148
23. Eldeberky, Y. Nonlinear transformation of wave spectra in the nearshore zone, Ph.D. thesis, Delft University of Technology, Department of Civil Engineering, The Netherlands, 1996.
24. Hasselmann, S.; Hasselmann, K.; Allender, J. H.; Barnett, T. P. Computations and Parameterizations of the Nonlinear Energy Transfer in a Gravity-Wave Spectrum. Part II: Parameterizations of the Nonlinear

- 354 Energy Transfer for Application in Wave Models. *J. Phys. Oceanogr.* **1985**, *15*, 1378-1391, DOI:  
355 10.1175/1520-0485(1985)015<1378:CAPOTN>2.0.CO;2.
- 356 25. Holthuijsen, L. H.; Herman, A.; Booij, N. Phase-decoupled refraction-diffraction for spectral wave models.  
357 *Coast. Eng.* **2003**, *49*, 291-305, DOI: [https://doi.org/10.1016/S0378-3839\(03\)00065-6](https://doi.org/10.1016/S0378-3839(03)00065-6)
- 358 26. SWAN team, Swan scientific and technical documentation, Delft University of Technology, 2018, 147p.